

Experimental Investigation of Anomalous Sputtering in the Vicinity of Microwave Neutralizer Cathode by Laser-induced Fluorescence Spectroscopy

IEPC-2024-545

*Presented at the 38th International Electric Propulsion Conference
Pierre Baudis Convention Center • Toulouse, France
June 23-28, 2024*

Ryudo Tsukizaki¹
Japan Aerospace Exploration Agency, Sagamihara, Kanagawa, 252-5210, Japan

Ryota Shirasawa²
The university of Tokyo, Bunkyo-ku, Tokyo, 113-8656, Japan

Marco Riccardo Inchingolo³
Universidad Carlos III de Madrid, Leganés, Madrid, 28911, Spain

Takato Morishita⁴ and Kazutaka Nishiyama⁴
Japan Aerospace Exploration Agency, Sagamihara, Kanagawa, 252-5210, Japan

Abstract: Throughout the in-space operation of the microwave gridded ion thrusters onboard Hayabusa2, the unexpected sputtering was observed. The phenomena resulted in the loss of the conductivity of the spacecraft surface and caused the malfunction of the cluster operation. To investigate the cause of the phenomenon, the laser-induced fluorescence spectroscopy is applied with a floated configuration. The measured IVDFs are compared with and without the cathode. The comparison revealed that only the plume from the neutralizer cathode consisting of two gaussian functions, low-energy and high energy, is the most probable cause of the sputtering. The high energetics ions are accelerated more than the neut-cathode operation voltage toward the spacecraft surface, whereas the IVDFs of CEX due to the cathode or ion source have the negligible effect on the sputtering.

I. Introduction

The microwave gridded ion thrusters “ $\mu 10$ ” have been developed by ISAS/JAXA to eliminate one of the lifetime limiters, a hollow cathode in the ion source.¹ The thrusters finished lifetime endurance test for the technological demonstration mission “HAYABUSA” in 1998 and 2002, with a time of 18,000h and 20,000h respectively.^{2,3} Despite the success of lifetime demonstration, the four-clustered thruster ended up its lifetime 12,000h to 15,000h in space.⁴ To investigate the lifetime difference between space and ground, Ohmichi et al conducted the failure tree analysis and concluded that it was due to the difference of thermal environment difference between the space operation and the ground operation.⁴ For the successor mission “Hayabusa2,” the neutralizer was enhanced the magnetic field and realized lower operation voltage, expecting lower sputtering rate. Also, Hayabusa2 firstly equipped two onboard environmental sensors “QCM” in the vicinity of the thruster to monitor the deposition rate deriving from the thruster. The authors developed the thrusters and launched the spacecraft in 2014 and made the asteroid sampling campaign and returned the spacecraft’s sample capsule in 2020 using the thrusters. Currently Hayabusa2 is under powered flight for the extended mission.⁵

However, through the space operation of the four-clustered microwave discharge ion thrusters “Hayabusa2,” the deposition was not observed but an anomalous sputtering was observed by the QCM sensors. The sputtering caused

the loss of a multi-layer thermal control film,⁶ resulting in the loss of conductivity of the surface of the spacecraft, and in the increase in the surface temperature. The loss of the electron conductivity affected the lifetime of the thrusters, because in order to equalize the neutralizer electron current in cluster operation of the thrusters, the microwave neutralizer current is controlled by PPU, emitting 3-10 mA excessively referring to each thruster's ion beam current. The excessive electron current must be recovered on the conductive surface. Currently only one thruster can be operational in the nominal mode. As for the other three thrusters, microwave neutralizer cathode must be floated to be operated, which is an off-nominal operation mode. This unexpected degradation resulted in the disability of the cluster operation of the thrusters after the end of the nominal mission since 2021. Now the spacecraft in the extended mission and is conducting powered cruising for the fly-by the asteroid 2001CC21 scheduled in 2026, and the rendezvous 1998KY26 in 2031.

This failure mode was analyzed by Nono et. al, and experimentally investigated and confirmed.⁷ Since the cause of sputtering is not investigated, we have applied the laser-induced fluorescence spectroscopy and visualized the ion movement around the neutralizer cathode.^{8,9} At first, the experimental set up is electrically grounded. The LIF measurements will be conducted with and without the neutralizer cathode to evaluate the effect of the cathode on the IVDFs. The IVDFs will be analyzed and decomposed to two gaussian functions, the high energy function around 30-40V, which only will appear with the cathode, and the low energy function around 0V. The high energy function exceeds the neutralizer cathode bias voltage, possibly resulting in the unexpected sputtering. As the second step, the thruster will be electrically isolated from the ground by using a Zenner diode. The ion velocity distribution functions (IVDFs) will be compared in the grounded configurations.

II. Experiment

A schematic of the “ $\mu 10$ ” microwave discharge gridded thruster is shown in Fig. 1. The thruster basically consists of a waveguide, a discharge chamber, a three-grid system and a neutralizer. Additionally, there is a microwave antenna and a propellant inlet at one end of the waveguide. The other end of the waveguide is connected to the discharge chamber (right side in Fig. 1) A microwave with a frequency of 4.25 GHz is transmitted through the waveguide to the discharge chamber. In the discharge chamber there are two rings of samarium-cobalt magnets. A propellant, Xenon, is injected via the inlets and flows into the discharge chamber. In the discharge chamber, electrons are accelerated by a mirror magnetic field and Electron Cyclotron Resonance heating. By subsequent electron-neutral and electron-ion collisions, ECR plasma is formed. The thrust force of the $\mu 10$ thruster was improved by changing the propellant injection location. In the flight model of HAYABUSA, it located at the end of the waveguide. In the improved model, it is also opened in the discharge chamber, and the propellant is distributed between the waveguide inlet and the discharge chamber inlets. A summary of the operational conditions is shown in Table 1.

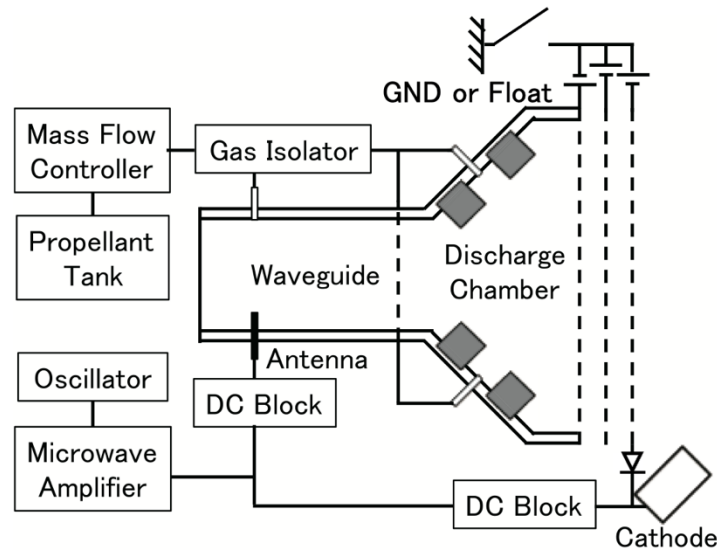


Fig. 1. The schematic of the $\mu 10$ microwave ion thruster.

Table 1. The Specifications of $\mu 10$ ion thruster.

Beam diameter (mm)	105
Microwave frequency (GHz)	4.25
Microwave power for ion source (W)	34
Microwave power for cathode (W)	8
Screen voltage (V)	1525
Accelerator voltage (V)	-370
Decelerator and neutralizer voltage (V)	~ -30
Thrust force (mN)	10.1
Beam current (mA)	170
Specific impulse (sec)	3000
Mass utilization efficiency (%)	85
Ion production cost (eV)	200
Ion source flow rate (mg/s)	0.27
Cathode flow rate (mg/s)	0.064

Fig. 2 shows the experimental setup of the laser induced fluorescence spectroscopy. In this measurement setup, a diode laser (DL100, Toptica Photonics AG), which emits 50mW laser light with a diameter of 2 mm, is used. The controller of the laser sweeps wavelengths (vacuum) ranging from 834.930 to 834.985 nm. The polarization of the emitted laser beam is changed using a half-wave plate, and the beam is then injected into an amplifier (BoosTA, Toptica Photonics AG). The amplifier boosts the power of the seed laser beam from 50 to 500 mW. Then, the laser beam is split into a wavemeter, a reference cell (Xe tube), and an optical fiber. Using an optical fiber feedthrough, the laser beam is injected to the 160-170 mA ion beam in the vacuum chamber. The laser beams sent to the reference cell and the optical fiber are modulated at 5.6 kHz by a chopper to improve the signal-to-noise ratio using a lock-in-amplifier (7270DSP, Signal Recovery, Inc.). Two photomultiplier detectors (H11462-031MOD, Hamamatsu Photonics K.K.) are used to detect the output laser beams. One is located on the optical bench for the reference cell, and the other is located on a linear stage inside the vacuum chamber. In front of the photomultipliers, 542 nm bandpass filters are included to improve the signal-to-noise ratio, and two convex lenses are used to collect the fluorescence signals. The probe laser and the detector are mounted on an automated linear stage. The laser is injected ± 45 degree to obtain the 2D velocity vector map. The measurement plane is set to the center of the guard ring shown in Fig. 2 on the right. Measurement points are written in Table 2.

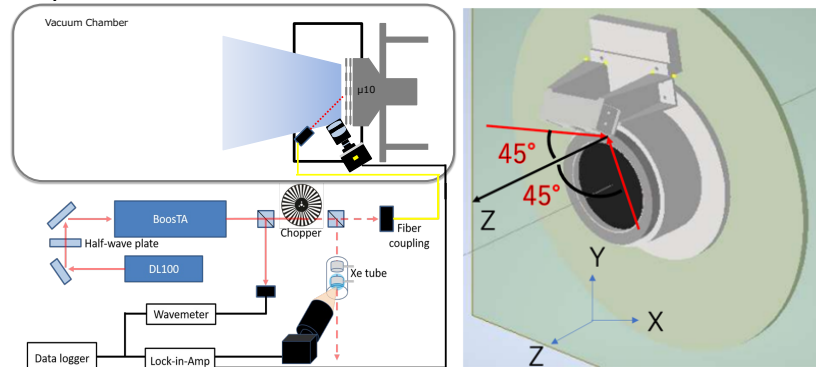


Fig. 2 The measurement set up of laser-induced fluorescence spectroscopy. (Left) The laser is injected to ± 45 degree for 2D map as shown on the right.

Table 2 Measurement points of LIF

X, mm	-10, 0, 10
Z, mm	10, 20, 30, 35, 40, 50, 60
Laser incident angle	$+45^\circ$, -45°

III. Results

The vector maps were successfully obtained, and the floated configuration is shown on the Left of Fig. 3. At $Z=10$ mm, the measurements were conducted, however, the signals of the fluoresce were non-detectable. From $Z=10$ to 35 mm, the averaged ion velocities are all negative values and resulted in the back streaming to the thruster guard ring. At $X=-10$ mm, $Z=35$ mm, the IVDFs are shown on the right of Fig. 3. Based on the assumption that IVDFs are consists of two gaussian functions, the experimental dataset is fitted by low energy function in blue and high energetic function in red. The cathode operation voltage was -28 V and the floated system voltage was -2.8 V, the energetic one distributed up to $-8,000$ m/s, equivalent to 43.8 V acceleration. Since the sputtering yield of Xe^+ to ITO exponentially increase, the high energetic ions would sputter the surface though its population is not so high.¹⁰ At $Z=40$ to 60 mm $X=0$ mm, the averaged ion velocities changed to positive values, ions go to down stream region. $Z=40$ to 60 mm $X=\pm 10$ mm, the z -directional velocities are closed to 0 and ions seem diffused based on x -directional velocities.

In case of the measurement without the neutralizer cathode, the IVDFs consists of only one function around the 0 eV, the authors predict that the instability of plume mode operation of the neutralizer cathode generated the enegetic ions, shown on the right of Fig. 3, and resulted in the anomalous sputtering observed in space.

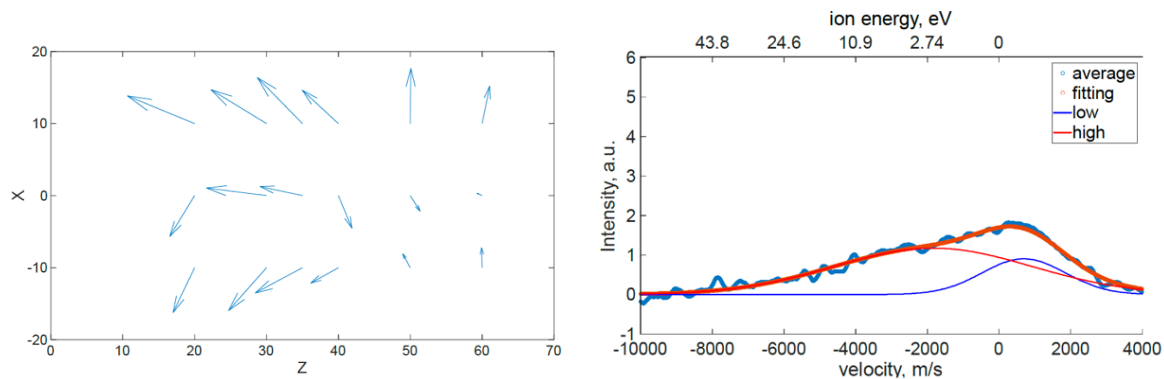


Fig. 3 The averaged ion velocity vector map on the left. Right shows the ion velocity distribution functions at $(x, z) = (-10, 35)$ in the floated configuration with $+45^\circ$ laser injection. Two gaussian functions are fitted to decompose the experimental data set. The higher energy function distributes more than 40 V, whereas the neutralizer cathode voltage was -28 V. The floated system voltage, i.e. the thruster guard ring, is -2.8 V.

IV. Conclusion

In this study, the LIF measurements campaign was successfully conducted to the microwave gridded ion thruster. The authors conclude as follows:

- From the surface to 35-40 mm downstream, the ions are accelerated to the upstream. The measured values are asymmetric with the axis of $X=0$ mm. Especially the region around $X=-10$ mm, $Z=35$ mm, the IVDFs are made of two gaussian functions, low and high energy.
- The high exegetic functions appeared only with the neutralizer cathode under electron beam extraction. Hence, the authors believe that CEX from the cathode or ion source are negligible.
- The above exegetic ion velocity function exceeds the cathode operation voltage. The plume mode operation instability, the oscillation of the potential, accelerate ions higher than the operation volatage toward the spacecraft surface.

Acknowledgments

I would like to express my gratitude to the Advanced Machining Technology Group of ISAS/JAXA for technical support. This work was financially supported by JSPS KAKENHI Grant Number 23H01614.

References

1. Kuninaka, H., and Satori, S., Development and Demonstration of a Cathode-less Electron Cyclotron Resonance Ion Thruster, Journal of Propulsion and Power, Vol. 14, No. 6, pp. 1022-1026, 1998.

2. Kuninaka, H., Nishiyama, K., Funaki, I., Yamada, T., Shimizu, Y., and Kawaguchi, J., Powered Flight of Electron Cyclotron Resonance Ion Engines on Hayabusa Explorer, *Journal of Propulsion and Power*, Vol. 23, No. 2, pp. 544-551, 2007.
3. Kuninaka, H., Nishiyama, K., Funaki, I., Yamada, T., Shimizu Y., and Kawaguchi, J., Deep Space Flight of Microwave Discharge Ion Engines onboard Hayabusa, *Journal of Space Technology and Science*, Vol. 22, No. 1, pp. 1-10, 2007.
4. Wataru Ohmichi and Hitoshi Kuninaka. Performance Degradation of a Spacecraft Electron Cyclotron Resonance Neutralizer and Its Mitigation, *Journal of Propulsion and Power*, Vol. 30, No. 5 (2014), pp. 1368-1372. doi: 10.2514/1.B35062
5. S. Sugita et al, The geomorphology, color, and thermal properties of Ryugu: Implications for parent-body processes, *Science*, aaw0422, (2019), doi: 10.1126/science.aaw0422
6. Tachikawa, S., Ohnishi, A., Nakamura, Y. and Okamoto, A. : Design and Optical Performance Evaluation of Smart Radiation Device with Multi-layer Coating, *Proceedings of 38th International Conference on Environmental Systems*, 2008-01-2152, 2008
7. A. Nono, et. al, <https://doi.org/10.1016/j.actaastro.2023.07.045>, *Acta Astronautica* 2023
8. Ryudo Tsukizaki, Yuta Yamamoto, Daiki Koda, Yamashita Yusuke, Kazutaka Nishiyama and Hitoshi Kuninaka, Azimuthal velocity measurement in the ion beam of a gridded ion thruster using laser-induced fluorescence spectroscopy, *2018 Plasma Sources Sci. Technol.* 27 015013
9. Takato Morishita, Ryudo Tsukizaki, Kazutaka Nishiyama, Hitoshi Kuninaka, Plasma parameters measured inside and outside a microwave-discharge-based plasma cathode using laser-induced fluorescence spectroscopy, *Journal of Applied Physics*, (2022), doi: 10.1063/5.0071294
10. John T. Yim, A survey of xenon ion sputter yield data and fits relevant to electric propulsion spacecraft integration, *IEPC-2017-060*